Available online at www.sciencedirect.com

ScienceDirect

Procedia CIRP 79 (2019) 153–158

www.elsevier.com/locate/procedia

12th CIRP Conference on Intelligent Computation in Manufacturing Engineering, 18-20 July 2018, Gulf of Naples, Italy

Fiber laser-MAG hybrid welding of DP/AISI 316 and TWIP/AISI 316 dissimilar weld

Giuseppe Casalino[a,*], Andrea Angelastro[a], Patrizia Perulli[a], Paolo Posa[a], Pasquale Russo Spena[b]

[a]DMMM, Politecnico di Bari, viale Japigia 182, Bari 70124, Italy

[b]Facoltà di Scienze e Tecnologie, piazza Università 5, Bolzano39100, Italy

* Corresponding author. Tel.: +39-080-5962753; fax: +39-080-5962788. *E-mail address:* giuseppe.casalino@poliba.it

Abstract

In this paper, TWinning-Induced Plasticity (TWIP), Dual Phase (DP) and austenitic stainless (AISI 316) steels were joined together by hybrid laser/arc welding with an austenitic steel filler. Microstructural and mechanical characterization of welded joints was carried out by optical microscopy, microhardness, tensile and bend tests. The heat affected zone (HAZ) at the TWIP side was fully austenitic and exhibited a grain coarsening; at the DP side, new martensite formed close to the fusion zone and other phase transformations occurred moving toward the base metal; at the AISI 316 side, stringers of untreated ferrite δ inside the austenitic matrix was observed. All the tensile welded specimens broke within austenitic stainless steel. TWIP/AISI 316 welds exhibited a greater tensile strength than DP/AISI 316 ones. The bending tests confirmed the ductility of both sorts of joints.

Peer-review under responsibility of the scientific committee of the 12th CIRP Conference on Intelligent Computation in Manufacturing Engineering.

Keywords: Twip steel; DP steel; AISI 316 steel; Hybrid laser arc welding; Dissimilar weld; Austenitic filler; Mechanical and microstructural characterization

1. Introduction

Nowadays, the automotive industry is continuously reducing vehicle weight to reduce fuel consumption and gas emissions, as well as to improve crashworthiness. For this reason, structural components and body panels are subjected to demands for lightweight and "tailor-made" multi-materials solutions, including the usage and assembling of advanced high strength steels (AHSSs).

AHSSs exhibit an excellent combination of mechanical properties, such as a remarkable tensile strength, high energy absorption, ductility, formability and good fatigue resistance [1, 2]. However, the material selection strategy in the automotive industry does not only aim to a weight reduction or make cars safer, but also everything is needed to produce a successful vehicle. In this context, joining different materials is of paramount importance.

High-manganese steels, namely TWinning Induced Plasticity steels (TWIP), have been recently proposed for car structural applications. These steels normally contain a high amount of manganese (15-30 % Mn), which retains a fully austenitic microstructure at room temperature. TWIP steels have an excellent strength and ductility due to the formation of mechanical twins during plastic deformation. Twins cause a high strain hardening, thus preventing necking and, in turn, postponing final fracture [5-8].

Other AHSSs like Dual Phase (DP) steels are used to fabricate car-body components (e.g., bumpers, side impact beams, etc.) [9]. DP steels combine a high tensile strength (usually from 500 to 1200 MPa) with a good formability [1, 10] because of a mixed microstructure of martensite dispersed in a soft ferritic matrix. Mechanical strength and ductility of DP steels can be designed by properly varying the volume fraction ratio of these two phases.

When corrosion resistance, durability and outward appearance are the main requirements, austenitic stainless steels are often chosen instead of other steel grades and protective coatings.

Austenitic stainless steels normally have excellent mechanical properties, both in terms of strength and ductility, which make them a promising solution for impact-resistance car body parts. Therefore, an increasing use of this steel grade is foreseen in the fabrication of structural components for the automotive industry.

2212-8271
Peer-review under responsibility of the scientific committee of the 12th CIRP Conference on Intelligent Computation in Manufacturing Engineering.
10.1016/j.procir.2019.02.035

A sheet-metal car body can have about 250 distinct parts, which are fabricated with different metal alloys. Therefore, joining of different metals is one of major tasks in vehicle production. Ytterbium fiber laser has demonstrated its capability of welding a variety of metal alloys in similar and dissimilar joints [11-14]. In many cases, it can be successfully coupled to an arc torch to offer some advantages like low heat input, high welding speed, arc stability, good process stability and weld penetration [15, 16].

This paper aims to assess the weldability of sheets of an AISI 316 stainless steel with a TWIP and DP steel. A fiber laser-MAG hybrid welding system was used. A filler material 316-Si/SKR-Si was employed to join the steels to avoid the formation of harmful Mn segregations and brittle martensite in the fusion zone of joints, as demonstrated by previous studies [1, 17]. The dissimilar welds were characterized in terms of microstructure, tensile properties, and bending behavior.

2. Experimental procedure

The sheets were 1.5 mm thick and they were welded in butt configuration. Table 1 and 2 show the chemical composition of TWIP, DP, and AISI 316 steels.

The heat source for the joining process was an Ytterbium Laser (IPG YLS-4000) combined with a MAG generator, with the laser beam being the leading welding source (see Fig. 1) [18]. The laser beam was delivered through a 200 μm diameter fiber with the maximum power of 4 kW and a continuous wavelength of 1070.6 nm.

The laser beam was focused on the sheet surface (Fig. 1) by a lens with a 250 mm focal distance. The MAG torch was tilted at an angle of 40 °. The two heat sources were distant 2 mm each other.

The shielding gas was a mixture of 87 % Ar and 13 % CO_2 to promote process stability and satisfactory joints.

Table 1. Chemical composition of TWIP and DP steels (% wt.).

Metal	C	Si	Mn	Cr	Mo	Al	Ti	B
TWIP	0.66	0.20	23.4	0.13	0.12	0.038	-	0.002
DP	0.09	0.21	1.65	0.43	-	0.03	0.003	-

Table 2. Chemical composition of AISI 316 (weight %).

C	Cr	Mn	Mo	Ni	P	S	Si	Fe
0.08	18	2	3	14	0.045	0.03	1	balance

Table 3 Chemical composition of austenitic filler.

Filler	C	Si	Mn	Cr	Mo	Ni	Cu	P
316L-Si/SKR-Si	0.016	0.82	1.65	18.1	2.57	12.33	0.03	0.023

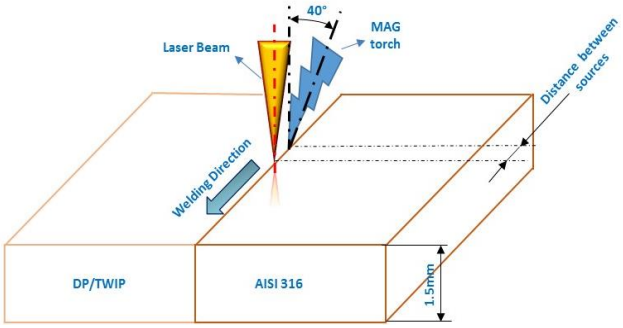

Fig. 1. Schematic configuration of laser-MAG hybrid welding.

Table 4. Process parameters of experimental test.

Laser power (W)	Laser speed (m/min)	Wire feed speed (m/min)	Current (A)	Voltage (V)
1500	2.4	8.6	94	20.2

An austenitic filler wire (316L-Si/SKR-Si) with a dimeter of 0.8 mm was used during the joining tests. Table 3 reports its chemical composition.

The process parameters used in the experimental tests are displayed in Table 4.

Optical microscopy (Nikon Epiphot 200, Nikon microscope) was performed on the cross section of the dissimilar welds to evaluate joint quality. Metallographic specimens were prepared with standard grinding and polishing techniques. The following etchants were used to reveal joints microstructures:

- Glyceregia solution, 15 ml HCl, 15 ml glycerol, 5 ml HNO_3 for AISI 316 and TWIP steels.
- Le Pera solution, 1 % vol. metabisulfite in distilled water and 4 % vol. picric acid in ethanol for DP steel.

The same metallographic samples were also used to carry out Vickers microhardness measurements (Affri, Induno Olona, VA, Italy) by using a load of 0.3 kg. Vickers micro-hardness indentations were carried out along the middle of the weld cross section thickness.

Tensile and bending tests were carried out to evaluate weld strength and formability.

3. Weld appearance and microstructure

The fusion zone (FZ) of the two dissimilar joints DP/AISI 316, Fig. 2, and TWIP/AISI 316, Fig. 3, does not show the presence of evident porosity or cracks.

FZ of TWIP/AISI 316 joint is made up of a dendritic structure, Fig. 4. As expected, dendrites proceed toward the weld centerline along the direction of heat transfer [19, 20]. Some small shrinkage cavities could be present in the interdendritic regions because the solidification process.

In the TWIP steels, shrinkage defects are highly expected owing to its high volumetric contraction during solidification [21-23].

DP/AISI 316 joints show a significant microstructural change in the DP HAZ due to the thermal cycle occurring during the joining

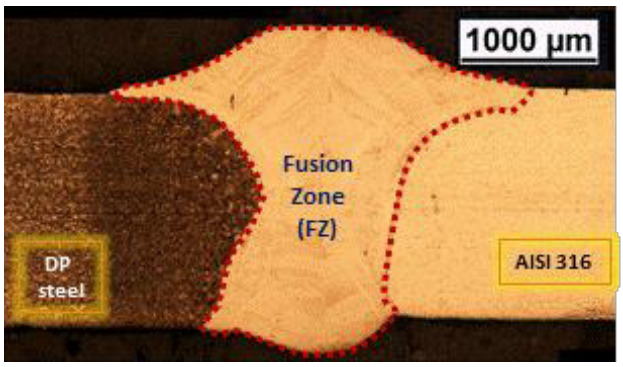

Fig. 2. Optical macrograph of the DP/AISI 316 joint cross section.

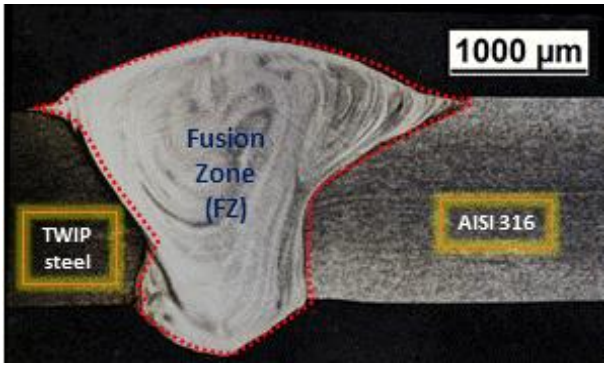

Fig. 3. Optical macrograph of the TWIP/AISI 316 joint cross section.

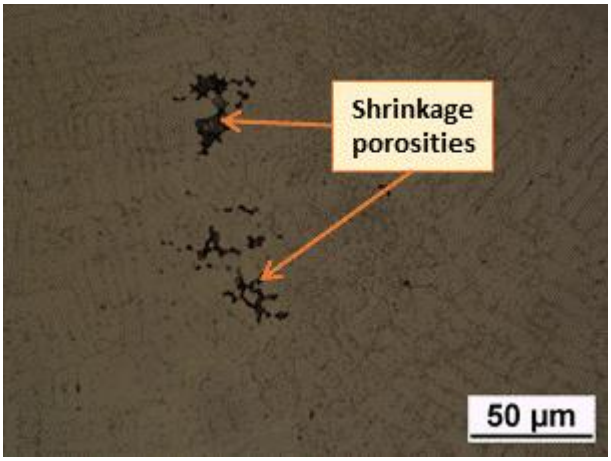

Fig. 4. Dendritic structure of the FZ and shrinkage cavities of TWIP/AISI 316 joints.

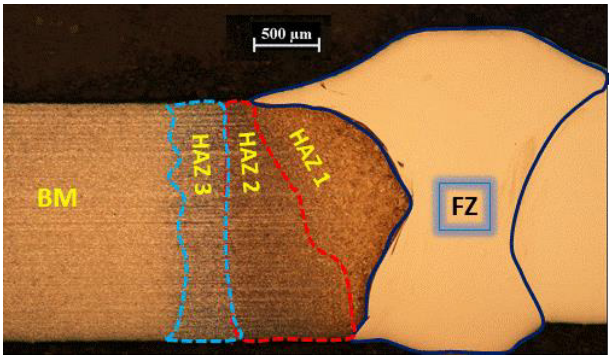

Fig. 5. FZ and different heat-affected zones in dissimilar joint DP/AISI 316. BM: base material.

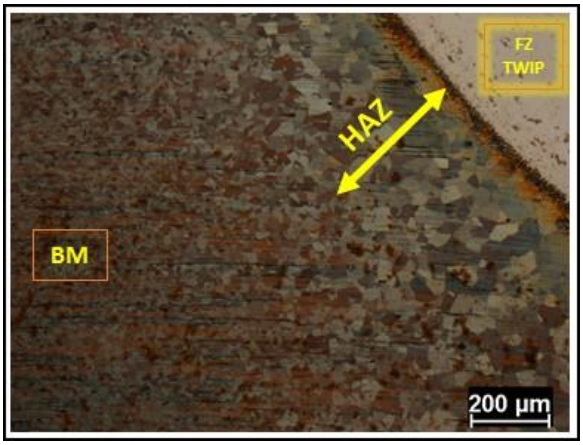

Fig. 6. Fine austenitic microstructure of the base material (BM) and grain coarsening at the HAZ TWIP side.

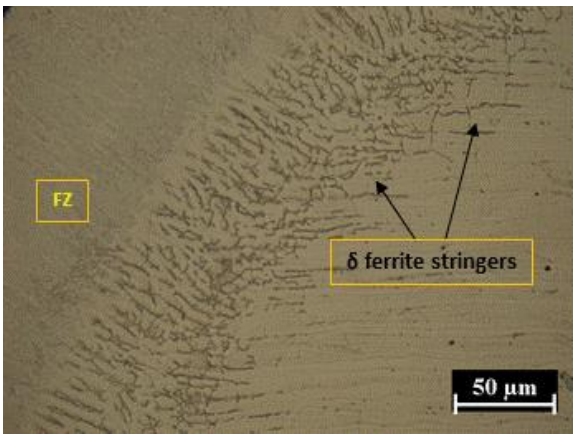

Fig. 7. Delta ferrite stringers at the HAZ AISI 316 side.

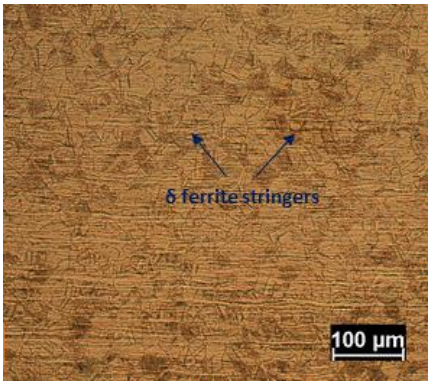

Fig. 8. Austenitic microstructure of AISI 316 steel with δ ferrite stringers.

As shown in Fig. 5, DP HAZ can be divided into three regions, as follows: HAZ 1, in which the martensite is the main constituent due to the high temperature close to the FZ and final rapid cooling; HAZ 2, which belongs to the inter-critical temperature range where steel partially austenitized and then quenched to martensite, whereas the original ferrite mainly softened; HAZ 3, which is the original martensite tempered and ferrite softened area, with the amount of martensite that decreases moving away from the fusion zone [24, 25].

TWIP steel exhibits a fine austenitic microstructure, while grain coarsening is clearly visible in its HAZ, Fig. 6.

The HAZ AISI 316 close to the fusion zone shows the presence of δ ferrite stringers (Fig. 7). It is known from the literature that the formation of δ ferrite stringers along HAZ grain boundaries hinders grain growth [28].

The formation of δ ferrite stringers could be caused by the migration of ferrite stabilizers, such as Cr and Mn, from the filler metal [28].

Fig. 8 shows the microstructure of AISI 316 stainless steel with the presence of δ ferrite stringers elongated along the rolling direction.

4. Weld microhardness

Weld microhardness varies notably throughout the DP/AISI 316 joint. The hardness of DP base metal was 215 ± 5 HV0.3. At the DP side, the hardness of the HAZ close to the FZ is significantly high, above 300 HV0.3, because of the presence of a fully martensitic microstructure.

Hardness reduces close to the base metal coherently with the microstructural transformations discussed previously, Fig. 9. The tempering of martensite in the HAZ 3 region has led to a hardness lower than that of the parent material.

In the FZ, hardness is a quite low due to its austenitic microstructure.

The hardness of TWIP base metal was 245 ± 5 HV0.3. The HAZ TWIP shows a lower microhardness than that of the base material due to the coarsening and softening of austenitic grains (Fig. 10).

The FZ of dissimilar joint TWIP/AISI 316 shows a low microhardness due to the austenitic microstructure, also promoted by the nature of the filler. The dissimilar joints exhibit the same hardness profile at the austenitic stainless steel.

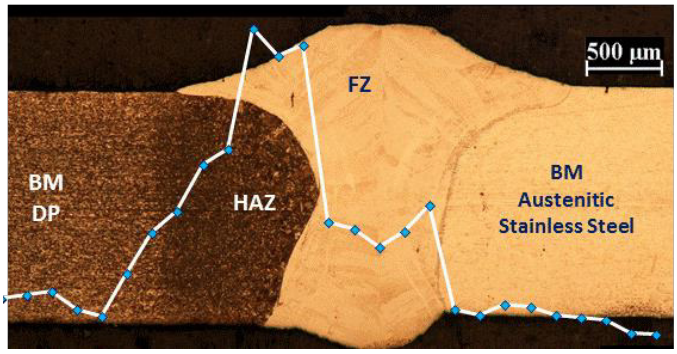

Fig. 9. Vickers Microhardness of the TWIP/AISI 316 joint.

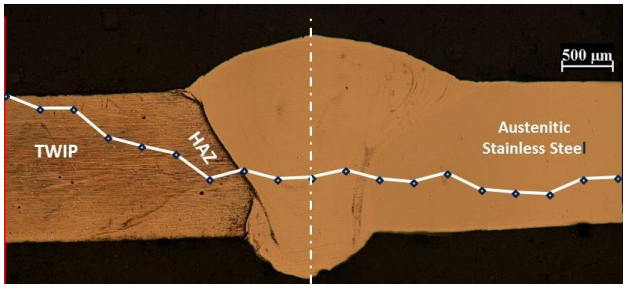

Fig. 10. TWIP-AISI 316 Vickers Microhardness [HV 0,3/15].

At the AISI 316 HAZ side, grain growth was limited, and hardness values became higher if compared with those of the base material (Figs. 9, 10). In this regard, it has been demonstrated that the formation of δ ferrite stringers along HAZ grain boundaries could contribute to restrict grain growth [28].

5. Tensile test

Tensile specimens were taken perpendicular to the weld seam. The sample width was 10 mm. The main mechanical properties resulting from the tensile tests performed on the dissimilar joints are displayed in Fig. 11 and listed in Table 5.

TWIP/AISI 316 weld exhibited a greater tensile strength and elongation at fracture than DP/AISI 316 one. The differences of UTS and elongation are not significant as the rupture regarded the same material, i.e. AISI 316. The experimental error is the responsible for that difference

All the tensile specimens broke within austenitic stainless steel, with the FZ and the HAZ exhibiting an adequate mechanical resistance. As shown in Fig. 12, welded samples fractured by a ductile rupture.

Strength and ductility (i.e. large elongation at fracture) of joints is ensured by the austenitic microstructure of the FZ and by twinning effects occurring during plastic deformation, which is basically promoted by the important levels of manganese and nickel in welds [30, 31].

These properties are of great interest in the automotive industry to improve vehicle performance in terms of safety and fuel consumption.

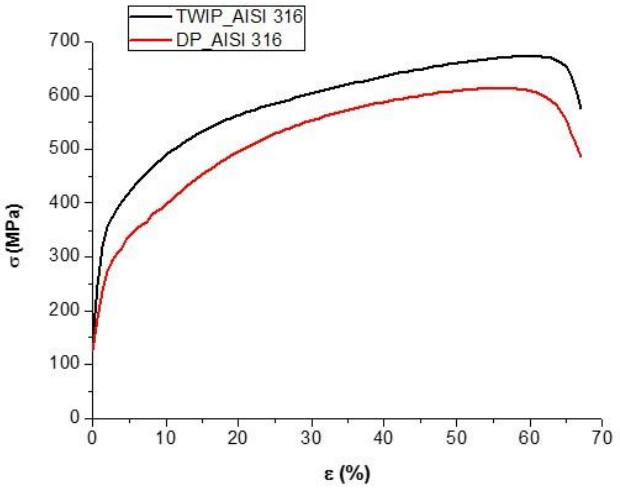

Fig. 11. Tensile curves of dissimilar specimens.

Fig. 12. TWIP/AISI cracked specimen.

Table 5. Tensile properties for dissimilar joints DP/AISI 316-TWIP/AISI 316. UTS: ultimate tensile strength, ε_{max}: elongation at fracture; σy: yield strength.

	UTS [Mpa]	ε_{max} [%]	σ_y [Mpa]
DP/AISI 316	614	61	325
TWIP/AISI 316	672	51	350
DP	880	15	490
TWIP	1050	40	420
AISI 316	640	50	320

6. Bending test

The dissimilar welded joints were subjected to three points bending test to evaluate the weld quality. The good bend behavior of welds has been confirmed by observations with naked eye, Fig. 13, and optical microscopy, Fig. 14 and 15. Both the joint types did not show defects on the weld surface after bending, even if they were subject to very high local deformations.

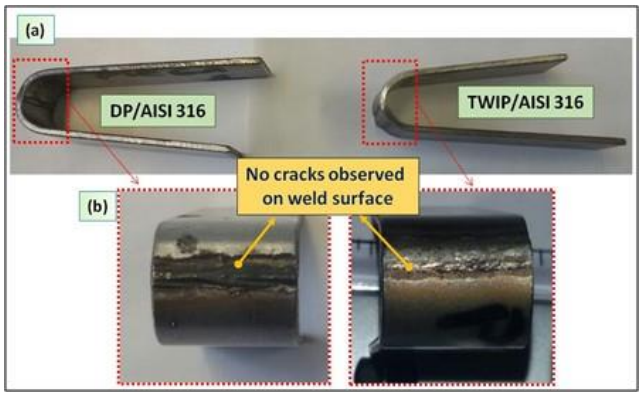

Fig. 13 (a) Joint appearance after the bend test . (b) Frontal views shows the absence of cracks on weld surface.

Fig. 14. Joint DP/AISI 316 cross section after bending.

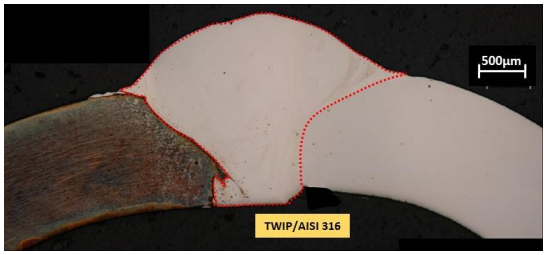

Fig. 15. Joint TWIP/ AISI 316 cross section after bending.

7. Conclusions

This work concerns weldability of TWIP and DP advanced high strength steels with an AISI316 austenitic stainless steel by means of hybrid MAG-laser welding in butt configuration. The microstructures, mechanical properties and bending of DP/AISI 316 and TWIP/AISI 316 dissimilar joints have been assessed and discussed. The main results are summarized as follows:

1) The HAZ at the TWIP side was fully austenitic and exhibited a grain coarsening. At the DP side new martensite formed close to the FZ, whose amount reduces moving away from the weldment. DP steel is more susceptible to the thermal cycle induced by the welding process than TWIP steel.

2) The HAZ at the DP side close to the FZ shows the maximum hardness, coherently with the presence of a fully martensitic microstructure. The HAZ of the TWIP steel exhibits a microhardness slightly lower than that of the corresponding base material, due to the softening and coarsening of austenitic grains during the welding process.

3) The FZ of TWIP/AISI 316 joint exhibit some small shrinkage porosities due to the solidification process.

4) TWIP/AISI 316 joints show a significant combination of strength and ductility, favored by twinning effect occurring during plastic deformation. DP/AISI joints also show a good mechanical strength and ductility, even though more limited than TWIP /AISI welds. All the tensile specimens broke within austenitic stainless steel.

5) The bending tests confirmed the attitude of the weld towards ductility. Both samples show defect-free surfaces and cross sections. Therefore, MAG-laser welding can be considered a valid welding technology to realize “tailor-made” solutions for welded sheets components in the automotive industry.

References

[1] Russo Spena P, D’Aiuto F, Matteis P, Scavino G. Dissimilar Arc Welding of Advanced High Strength Car-Body Steel Sheets. Journal of Materials Engineering and Performance 2014; 23: 3949–3956.

[2] Cappelli F, Boneschi V, Viganò P. Stainless steel. A new strucural automotive material. 9th International conference & Exhibitions, Florence ATA 2005.

[3] Rüsinga CJ, Lambersb HG, Lackmannc J, Frehnc A, Nageld M, Schapera M, Maiere HJ, Niendorfa T. Property optimization for TWIP steels – Effect of pre-deformation temperature on fatigue properties, International Conference on Martensitic Transformations, ICOMAT-2014, Proceedings 2S 2015; S681 – S685.

[4] Angelastro A, Casalino G, Perulli P, Russo Spena P. Weldability of TWIP and DP steel dissimilar joint by laser arc hybrid welding with austenitic filler. Procedia CIRP 2018; 67:607-611

[5] Russo Spena P, De Maddis M, Lombardi F, Rossini M. Dissimilar resistance spot welding of Q&P and TWIP steel sheets. Materials and Manufacturing Processes 2016; 31 : 291-299.

[6] Cornette D, Cugy P, Hildenbrand A, Bouzekri M, Lovato G. Ultra High Strength FeMn TWIP Steels for automotive safety parts. Revue de Métallurgie 2005; 102: 905-918.

[7] Jun JH, Choi CS. The influence of Mn content on microstructure and damping capacity in Fe-(17–23)% Mn alloys. Materials Science and Engineering: A 1998; 252: 133-138.

[8] Tomota Y, Strum M, Morris JW. Microstructural dependence of Fe-high Mn tensile behavior. Metallurgical and Materials Transactions 1986; 17:537–547.

[9] Rossini M, Russo Spena P, Cortes L, Matteis P, Firrao D. Investigation on dissimilar laser welding of advanced high strength steel sheets for the automotive industry. Materials Science and Engineering: A 2015; 628: 288–296.
[10] Evin E, Miroslav T. The Influence of Laser Welding on the Mechanical Properties of Dual Phase and Trip Steels. Metals 2017; 7(7) 239.
[11] Casalino G, Mortello M, Campanelli SL. Ytterbium fiber laser welding of Ti6Al4V alloy. Journal of Manufacturing Processes 2015; 20: 250-256.
[12] Casalino G, Mortello M, Peyre P. Yb-YAG laser offset welding of AA5754 and T40 butt joint. Journal of Materials Processing Technology 2015; 223:139-149.
[13] Casalino G, Mortello M. Modeling and experimental analysis of fiber laser offset welding of Al-Ti butt joints. International Journal of Advanced Manufacturing Technology 2016; 83:89-98.
[14] Casalino G, Guglielmi P, Lorusso VD, Mortello M, Peyre P, Sorgente D. Laser offset welding of AZ31B magnesium alloy to 316 stainless steel. Journal of Materials Processing Technology 2017; 242:49-59.
[15] Casalino G, Leo P, Mortello M, Perulli P, Varone A. Effects of Laser Offset and Hybrid Welding on Microstructure and IMC in Fe–Al Dissimilar Welding. Metals 2017; 7: 282.
[16] Zhang K, Lei Z, Chen Y, Liu M, Liu Y. Microstructure characteristics and mechanical properties of laser-TIG hybrid welded dissimilar joints of Ti–22Al–27Nb and TA15, Optics & Laser Technology 2015; 73 : 139-145.
[17] Russo Spena P, Matteis P, Scavino G. Dissimilar Metal Active Gas Welding of TWIP and DP Steel Sheets. Steel Reserch Internetional Journal 2015; 495-501.
[18] Casalino G, Campanelli SL, Maso UD, Ludovico AD. Arc leading versus laser leading in the hybrid welding of aluminium alloy using a fiber laser. 2013 Procedia CIRP, 2013, 12:151-156.
[19] Messler RW. Principles of Welding; Wiley-VCH, John Wiley & Sons, Inc.: Singapore, 2004.
[20] Porter DA, Easterling KE. Phase Transformations in Metals and Alloys; Chapman & Hall: London, UK, 1992
[21] Razmpoosh MH, Shamanian M, Esmailzadeh M. The microstructural evolution and mechanical properties of resistance spot welded Fe–31Mn–3Al–3Si TWIP steel. Material Design 2015; 67: 571–576.
[22] Holovenko O, Ienco MG, Pastore E, Pinasco MR, Matteis P, Scavino G, Firrao D. Microstructural and mechanical characterization of welded joints on innovative high-strength steels. La Metallurgia Italiana 2013; 3 : 3-12.
[23] Wang T, Zhang M, Xiong W, Liu R, Shi W, Li L. Microstructure and tensile properties of the laser welded TWIP steel and the deformation behavior of the fusion zone. Material Design 2015; 83: 103–111.
[24] Farabi N, Chena DL, Zhou Y. Microstructure and mechanical properties of laser welded dissimilar DP600/DP980 dual-phase steel joints. Journal of Alloys and Compounds 2011; 509: 982–989.
[25] Xia M, Biro E, Tian Z, Zhou YN. Effects of Heat Input and Martensite on HAZ Softening in Laser Welding of Dual Phase Steels. ISIJ International 2008; 48: 809–814.
[26] Mujicaa L, Weber S¸ Pinto H, Thomye C, Vollertsene F. Microstructure and mechanical properties of laser-welded joints of TWIP and TRIP steels. Materials Science and Engineering: A 2010; 527: 2071–2078.
[27] Mujica L, Weber S, Pinto H, Thomy C, Vollertsen F. Microstructure and mechanical properties of laser-welded joints of TWIP and TRIP steels. Materials Science and Engineering: A 2010; 527: 2071-2078.
[28] Arivarasua, M, Kasinatha DR, Natarajana A. Effect of Continuous and Pulsed Current on the Metallurgical and Mechanical Properties of Gas Tungsten Arc Welded AISI 4340 Aeronautical and AISI 304 L Austenitic Stainless Steel Dissimilar Joints. Materials Research 2015; 18: 59-77
[29] Kunishige K, Yamauchi N, Taka T, Nagao N. Softening in Weld Heat Affected Zone of Dual Phase Steel Sheet for Automotive Wheel Rim. SAE International Congress and Exposition in Detroit, Michigan USA; SAE; 1983.
[30] Kusakin PS, Kaibyshev RO. Hight-Mn Twinning-Induced Plasticity Steels: Microstructure and Mechanical Properties. Reviews on advanced materials science 2016; 44: 326-360.
[31] Casalino G, Angelastro A, Perulli P, Casavola C, Moramarco V. Study on the fiber laser/TIG weldability of AISI 304 and AISI 410 dissimilar weld. Journal of Manufacturing Processes 2018; 35 : 216-225.